Multi-Band Antenna Array Geometry Impact on Array Interpolation

Marco A. M. Marinho, Alexey Vinel, *Halmstad University, Sweden*
Per Gustafson, *Gutec AB, Sweden*
Felix Antreich, *Aeronautics Technology Institute, Brazil*
Stefano Caizzone, *German Aerospace Agency, Germany*

BIOGRAPHY

Marco A. M. Marinho is a postdoctoral researcher with Halmstad University in Sweden, focusing on localization and array signal processing. He previously worked with the Institute of Communications and Navigation of the German Aerospace Center (DLR).

Alexey Vinel is a Professor with the School of Information Technology, Halmstad University, Halmstad, Sweden, since 2015. His research interests include wireless communications, vehicular networking, and autonomous driving.

Per Gustafson is the chairman at Gutec AB. He is an experienced electromagnetics and electronics designer with a wide technical experience, and abilities as integrator. His research interests include electromagnetic design, antennas, radiation effects in electronics, electronics design, system design, and manufacturability.

Felix Antreich is a Professor with the Department of Telecommunications in the Division of Electronics Engineering of the Aeronautics Institute of Technology (ITA), Brazil. His research interests include sensor array signal processing for global navigation satellite systems (GNSS) and wireless communications, estimation theory, wireless sensor networks, positioning, localization, and signal design for synchronization.

Stefano Caizzone received an M.Sc. degree in telecommunications engineering and a Ph.D. degree in geoinformation from the University of Rome "Tor Vergata," Italy, in 2009 and 2015, respectively. Since 2010, he has been with the antenna group of DLR's Institute of Communications and Navigation, where he is responsible for the development of innovative miniaturized antennas.

ABSTRACT

Multi-band or multi-frequency antennas have become essential for many Global Navigation Satellite Systems (GNSS) applications. These antennas allow a receiver to simultaneously receive from multiple bands, which is essential for ionosphere corrections, can help mitigating multipath induced biases, and improve overall system availability. Another advancement that has recently attracted attention in the GNSS community is the usage of antenna arrays at the receiver. These arrays can be used to enhance system performance in multiple ways such as using beamforming to null out interferers or multipath components or enable a receiver to estimate its attitude while relying solely on received GNSS signals. While both multi-band antennas and antenna arrays offer attractive advantages for precise GNSS positioning, merging such systems on a single receiver can be challenging. Antenna arrays have their performance largely dictated by their geometries and the spacing between antenna elements. This spacing is defined with respect to the frequency of the signal that is received at the antenna array. If the spacing is too large the receiver will suffer from inaccuracy introduced by ambiguities that will be present when trying to filter out undesired signals or when trying to estimate the direction of arrival of received signals. If the spacing is too small, the total array directivity will be lower, which will lead to more biased direction of arrival estimations or to beamformers with lobes that are too broad to filter out undesired signals. The relationship between frequency and geometry makes it impossible to create a multi-band antenna array that is optimal for every frequency received, as optimizing one frequency will inevitably lead to performance degradation in the remaining ones. To tackle this issue, a technique known as array interpolation can be employed. Array interpolation consists of creating a mathematical transformation that projects the signal received at a real and imperfect array onto an ideal and abstract receiver. A different array interpolation can be constructed for each individual frequency received at the array. Thus, array interpolation can be a valuable tool for allowing multi-band antenna arrays to achieve high performance over the entire range of frequencies they are designed to receive. This work studies the effects of optimizing antenna array geometries for a given frequency band while applying array interpolation over the array response for the remaining frequency bands. The performance of multiple array interpolation methods is verified, and the tradeoffs between performance and computational complexity is studied.

I. INTRODUCTION

The availability of multiple Global Navigation Satellite Systems (GNSS), such as GPS, GLONASS, GALILEO, and BeiDou make the usage of multi-band antennas very attractive. These antennas allow receivers to process signals from multiple systems at the same time, leading to improved availability and improving overall system performance by providing improved geometry or helping to mitigate the impacts of multipath. The design of such antennas has already been studied and shows that it is possible to design small antennas that offer sufficient separation between the multiple bands [1].

Another technology that has recently made its way into GNSS receivers is the usage of antenna arrays. Antenna arrays can provide a myriad of benefits for GNSS applications. Spatial filtering can be employed to null out strong multipath components, spoofers, or jammers [2], allowing the receiver to provide improved reliability under challenging scenarios. While antenna arrays are usually bulky, limiting their applicability, compact multi-band solutions can be built, limiting the footprint, and allowing array signal processing to be employed in GNSS receivers [3].

The application of multi-band antennas and antenna arrays is, however, not without its challenges. The performance of antenna arrays is dictated largely by its geometry, in special by its element separation [4]. The optimal inner element separation is given as a fraction of the wavelength of the incoming signal. Therefore, for multi-band arrays, it is impossible to optimize the array geometry for more than one frequency band at a time, as optimizing for one given frequency would result in degrading the performance of another. Furthermore, other constrains might affect the array geometry, such as limited available space or having to conform to other practical aspects of the environment it is placed in.

To handle the limitations with respect to geometry optimization of multi-band antenna arrays, array interpolation can be employed. Array interpolation consists of mapping an arbitrary array response onto the desired (ideal) response [5, 6]. This mapping is done by obtaining a mathematical transformation capable translating the real response into the desired one. This allows the application of multiple important array signal processing techniques [7, 8] to arrays that are not optimized for any given frequency.

In this work the performance of array interpolation for multi-band GNSS antenna arrays is studied. Due to the relatively large difference between the center frequency of multiple bands such as L1 and L2 or L5, optimizing an array for a given frequency band will largely degrade its performance over the remaining ones. Thus, this work considers the trade-off between the performance of multiple frequency bands, presenting a study on array inner element separation versus direction of arrival estimation bias over all frequency bands of the array.

The remainder of this work is organized in four sections. In Section II. the data model used in this work is presented and detailed. Section III. presents a review on the basic concepts of array interpolation. Section IV. presents a set of numerical simulations highlighting array interpolation performance over multi-band arrays and aiming to find the optimal trade off. Lastly, in Section V., conclusions are drawn.

II. DATA MODEL

Assuming a set of d wavefronts impinging onto an antenna array composed of M antenna elements, the received baseband signal can be expressed in matrix form as

$$\mathbf{X} = \boldsymbol{A}\boldsymbol{S} + \boldsymbol{N} \in \mathbb{C}^{M\times N}, \tag{1}$$

where $\boldsymbol{S} \in \mathbb{C}^{d\times N}$ is the matrix containing the N symbols transmitted by each of the d sources, $\boldsymbol{N} \in \mathbb{C}^{M\times N}$ is the noise matrix with its entries drawn from $\mathcal{CN}(0, \sigma_n^2)$, and

$$\boldsymbol{A} = [\boldsymbol{a}(\theta_1), \boldsymbol{a}(\theta_2), ..., \boldsymbol{a}(\theta_d)] \in \mathbb{C}^{M\times d}, \tag{2}$$

where θ_i is the azimuth angle of the $i-\mathrm{th}$ signal and $\boldsymbol{a}(\theta_i) \in \mathbb{C}^{M\times 1}$ is the array response (empirical measurement).

The received signal covariance matrix $\boldsymbol{R_{XX}} \in \mathbb{C}^{M\times M}$ is given by

$$\boldsymbol{R_{XX}} = \mathrm{E}\{\boldsymbol{X}\boldsymbol{X}^{\mathrm{H}}\} = \boldsymbol{A}\boldsymbol{R_{SS}}\boldsymbol{A}^{\mathrm{H}} + \boldsymbol{R_{NN}}, \tag{3}$$

where $(\boldsymbol{.})^{\mathrm{H}}$ stands for the conjugate transposition, and

$$\boldsymbol{R_{SS}} = \begin{bmatrix} \sigma_1^2 & \gamma_{1,2}\sigma_1\sigma_2 & \cdots & \gamma_{1,d}\sigma_1\sigma_d \\ \gamma_{1,2}^*\sigma_1\sigma_2 & \sigma_2^2 & & \vdots \\ \vdots & & \ddots & \\ \gamma_{1,d}^*\sigma_1\sigma_d & \gamma_{2,d}^*\sigma_2\sigma_d & \cdots & \sigma_d^2 \end{bmatrix}, \tag{4}$$

where σ_i^2 is the power of the $i-\mathrm{th}$ signal and $\gamma_{a,b} \in \mathbb{C}$, $|\gamma_{a,b}| \leq 1$ is the cross correlation coefficient between signals a and b. $\boldsymbol{R_{NN}} \in \mathbb{C}^{M \times M}$ is a matrix with σ_n^2 over its diagonal and zeros elsewhere. An estimate of the signal covariance matrix can be obtained by

$$\hat{\boldsymbol{R}}_{\boldsymbol{XX}} = \frac{\boldsymbol{X}\boldsymbol{X}^{\mathrm{H}}}{N}. \tag{5}$$

III. ARRAY INTERPOLATION

Array interpolation, also know as array mapping, aims to predict what would be the data received at an array with a desired specific geometry based on the data received at a real array with arbitrary geometry or response. Figure 1 present a graphical example of what array interpolation aims to achieve.

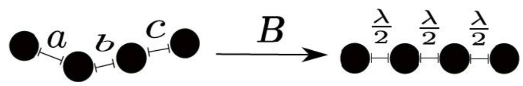

Figure 1: Graphical representation of array interpolation

Array interpolation seeks to find a transformation matrix $\boldsymbol{B}$ that satisfies

$$\boldsymbol{B}\boldsymbol{A} = \bar{\boldsymbol{A}}, \tag{6}$$

where $\boldsymbol{A}$ and $\bar{\boldsymbol{A}}$ are the real and desired array steering matrices respectively. Assuming the receiver has no prior information about the DOA of the received signals, $\boldsymbol{A}$ and $\bar{\boldsymbol{A}}$ are constructed by dividing the field of view of the array into W continuous regions, called sectors, with upper bound u_w and lower bound l_w. The region $[l_w, u_w]$ is then discretized according to

$$\mathcal{S}_w = [l_w, l_w + \Delta, ..., u_w - \Delta, u_w], \tag{7}$$

where Δ is the angular resolution of the transformation. These angles are used to generate the respective set of steering vectors and construct $\boldsymbol{A}$ and $\bar{\boldsymbol{A}}$ according to

$$\boldsymbol{A}_{\mathcal{S}_w} = [\boldsymbol{a}(l_w), \boldsymbol{a}(l_w + \Delta), ..., \boldsymbol{a}(u_w - \Delta), \boldsymbol{a}(u_w)] \in \mathbb{C}^{M \times \frac{u_w - l_w}{\Delta}},$$

$$\bar{\boldsymbol{A}}_{\mathcal{S}_w} = [\bar{\boldsymbol{a}}(l_w), \bar{\boldsymbol{a}}(l_w + \Delta), ..., \bar{\boldsymbol{a}}(u_w - \Delta), \bar{\boldsymbol{a}}(u_w)] \in \mathbb{C}^{M \times \frac{u_w - l_w}{\Delta}},$$

where M is the total number of antennas present at the array. The transformation is usually not perfect since there are not enough degrees of freedom to transform the entire desired sector. $\boldsymbol{B}$ is obtained as the least squares fit between the transformed response $\boldsymbol{B}\boldsymbol{A}_{\mathcal{S}_w}$ and the desired response $\bar{\boldsymbol{A}}_{\mathcal{S}_w}$

$$\boldsymbol{B} = \bar{\boldsymbol{A}}_{\mathcal{S}_w} \boldsymbol{A}_{\mathcal{S}_w}^{\dagger} \in \mathbb{C}^{M \times M}, \tag{8}$$

where $(\cdot)^{\dagger}$ is the pseudo inverse of the matrix. To access the precision of the transformation the Frobenius norm of the errors matrix $\boldsymbol{B}\boldsymbol{A}_{\mathcal{S}_w} - \bar{\boldsymbol{A}}_{\mathcal{S}_w}$ is compared with the Frobenius norm of the desired response steering matrix $\bar{\boldsymbol{A}}_{\mathcal{S}_w}$. The error of the transform is defined as

$$\epsilon(\mathcal{S}_w) = \frac{\left\|\bar{\boldsymbol{A}}_{\mathcal{S}_w} - \boldsymbol{B}\boldsymbol{A}_{\mathcal{S}_w}\right\|_{\mathrm{F}}}{\left\|\bar{\boldsymbol{A}}_{\mathcal{S}_w}\right\|_{\mathrm{F}}} \in \mathbb{R}^{+}. \tag{9}$$

Large transformation errors will result in a large bias in the final DOA estimates.

With $\boldsymbol{B}$ at hand the data can be transformed by

$$\bar{\boldsymbol{X}} = \boldsymbol{B}\boldsymbol{X}. \tag{10}$$

The transformed covariance is then equivalent to

$$\bar{\boldsymbol{R}}_{\boldsymbol{XX}} = \frac{\boldsymbol{B}\boldsymbol{X}(\boldsymbol{B}\boldsymbol{X})^{\mathrm{H}}}{N} = \frac{\boldsymbol{B}\boldsymbol{X}\boldsymbol{X}^{\mathrm{H}}\boldsymbol{B}^{\mathrm{H}}}{N} = \boldsymbol{B}\hat{\boldsymbol{R}}_{\boldsymbol{XX}}\boldsymbol{B}^{\mathrm{H}}. \tag{11}$$

From (11) it is easy to see that the transformation matrix can instead be applied directly to the covariance matrix. By plugging (4) into (11) we have

$$\begin{aligned}\bar{\boldsymbol{R}}_{\boldsymbol{XX}} &= \boldsymbol{B}\boldsymbol{A}\boldsymbol{R}_{\boldsymbol{SS}}\boldsymbol{A}^{\mathrm{H}}\boldsymbol{B}^{\mathrm{H}} + \boldsymbol{B}\boldsymbol{R}_{\boldsymbol{NN}}\boldsymbol{B}^{\mathrm{H}} \\ &= \bar{\boldsymbol{A}}\boldsymbol{R}_{\boldsymbol{SS}}\bar{\boldsymbol{A}}^{\mathrm{H}} + \boldsymbol{B}\boldsymbol{R}_{\boldsymbol{NN}}\boldsymbol{B}^{\mathrm{H}}.\end{aligned} \tag{12}$$

Thus, although the transformation transforms $\boldsymbol{A}$ into $\bar{\boldsymbol{A}}$ as desired it changes the characteristics of $\boldsymbol{R}_{\boldsymbol{NN}}$. If the noise was previously white it becomes colored or, if the noise was already colored, it changes its color. Since most of the methods in the literature assume that $\boldsymbol{R}_{\boldsymbol{NN}} = \sigma_n^2\boldsymbol{I}$, i.e, white noise, the next step used in classical interpolation is a noise whitening step to restore the diagonal characteristic of $\boldsymbol{R}_{\boldsymbol{NN}}$

$$\bar{\boldsymbol{R}}_{\boldsymbol{XX}} = \bar{\boldsymbol{R}}_{\boldsymbol{NN}}^{-\frac{1}{2}}\bar{\boldsymbol{R}}_{\boldsymbol{XX}}\bar{\boldsymbol{R}}_{\boldsymbol{NN}}^{-\frac{\mathrm{H}}{2}}, \tag{13}$$

where $\bar{\boldsymbol{R}}_{\boldsymbol{NN}} = \boldsymbol{B}\boldsymbol{R}_{\boldsymbol{NN}}\boldsymbol{B}^{\mathrm{H}}$. This operation, however, tends to increase bias due to the possible ill conditioning of the original noise covariance and, although it diagonalizes o the noise covariance term again, it affects the signal covariance.

IV. ARRAY INTERPOLATION PERFORMANCE FOR MULTI-BAND ARRAYS

To study the effects of array interpolation on multi-band antenna arrays, a numerical set of simulations was performed to measure the direction of arrival estimation performance over multiple frequency bands. For this set of simulations an array composed of $M = 6$ elements in considered. $\hat{\boldsymbol{R}}_{\boldsymbol{XX}}$ is obtained using $N = 200$ snapshots and the Root Mean Squared Error (RMSE) is calculated with respect to 1000 Mont Carlo simulations. We assume three signals impinging from $\theta_1 = 45$, $\theta_2 = 38°$, and $\theta_3 = 15°$, the given RMSE is

$$\mathrm{RMSE} = \sqrt{\frac{1}{K}\sum_{k=1}^{K}\left((\hat{\theta}_{1,k} - \theta_1)^2 + (\hat{\theta}_{2,k} - \theta_2)^2 + (\hat{\theta}_{3,k} - \theta_3)^2\right)}, \tag{14}$$

where $\hat{\theta}_i$ is the estimate of θ_i. The Signal to Noise Ratio (SNR) is set at 10 dB, and is defined as

$$\mathrm{SNR} = \frac{\sigma_1^2}{\sigma_{\mathrm{n}}^2} = \frac{\sigma_2^2}{\sigma_{\mathrm{n}}^2} = \frac{\sigma_3^2}{\sigma_{\mathrm{n}}^2}. \tag{15}$$

To assess the performance of the proposed method under demanding conditions the set of transmitted signals is highly correlated. The wavefronts impinging from θ_1 and θ_2 are correlated with correlation coefficient $\rho = 1$ and correlated to the wavefront impinging from θ_3 with $\rho = 0.8$, the FBA-SPS approach proposed in [9] is used and DOA estimation is performed using the TLS ESPRIT and the generalized eigen-value decomposition to cope with the noise coloring introduced by the transformation.

The first set of simulations, presented in Figure 2, shows the direction of arrival performance of the array for frequency bands L1, L2 and L5. The dashed lines represent the performance of the array when no array interpolation is used, while the solid lines present the performance of the array after array interpolation. The results highlight the fact that, unless the optimal separation of half of the wavelength is used, array interpolation provides improved performance. At the left side of the curve it is possible to notice that the performance for an L1 signal is maximal when the inner element separation is approximately 9.5 cm, what is, half of the wavelength of an L1 signal. The same effect can be seen at the right side of the curve for the L2 and L5 signals. Since these signals are much closer to each other in the frequency domain, their optimal element separation is also similar, being approximately 12 cm for the L2 signal and 12.7 for the L5 signal.

It is clear from the results that optimizing for L1 will degrade the performance of the array over the L2 and L5 frequency bands, and vice versa. However, when applying array interpolation, a compromised can be reached, by setting the inner element separation of the array to approximately 11 cm it is possible to achieve direction of arrival estimation accuracy within one degree.

Figure 3 presents the combined performance of the array for all three frequency bands versus the inner element separation. The combined performance is shown to be greatest at an inner element separation of approximately 12.3 cm. However, these results are skewed by the fact that the L2 and L5 frequencies have a relatively similar optimal inner element separation of 12 and 12.7 cm respectively. Thus, when dealing with the combined performance, it might be necessary to weight the performance of the multiple frequency bands according to their respective importance to the receiver and application at hand.

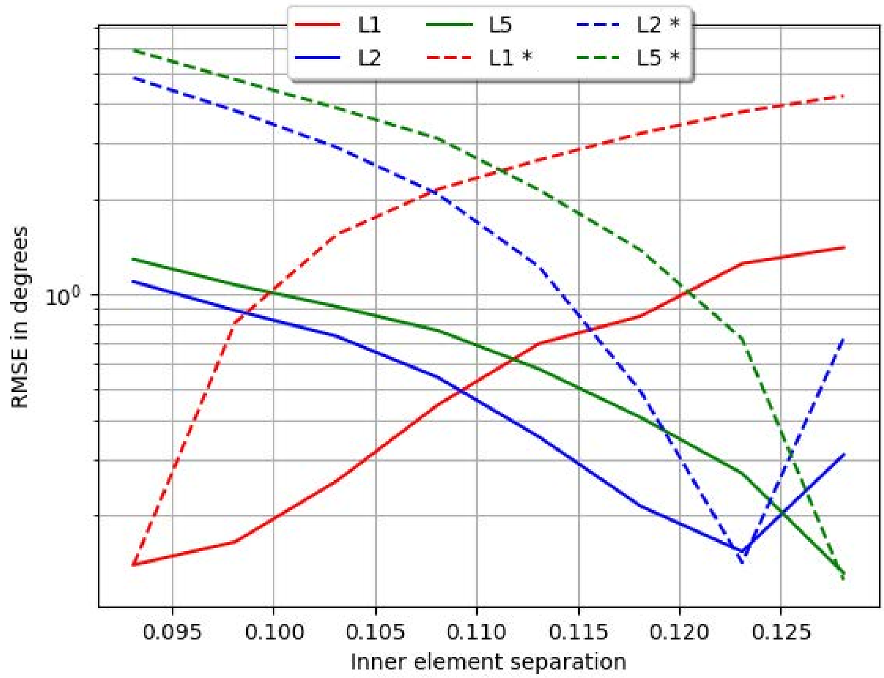

Figure 2: Direction of arrival estimation performance for multiple frequency bands versus inner element separation in meters

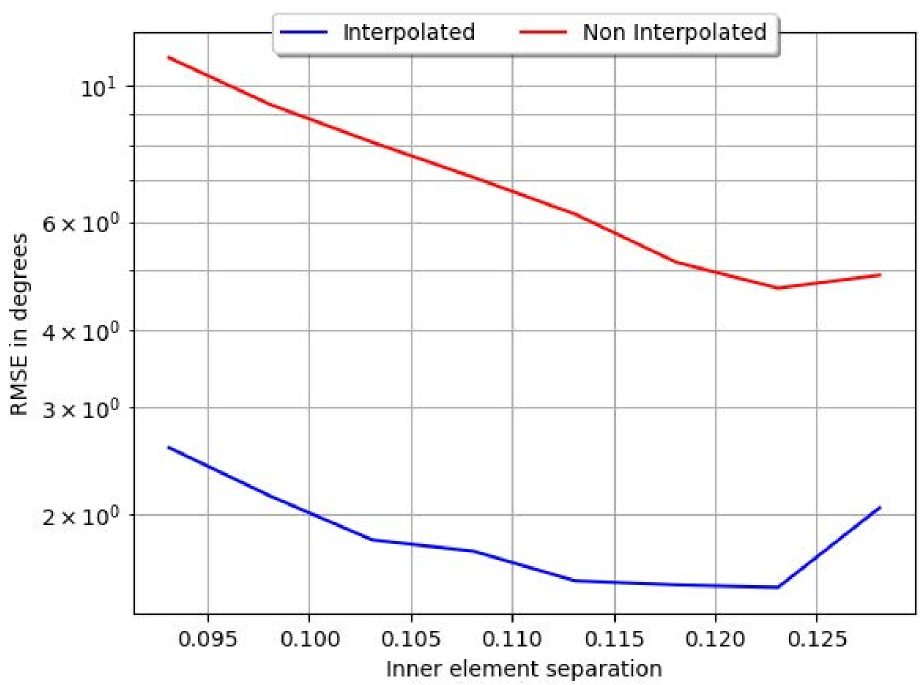

Figure 3: Combined direction of arrival estimation performance versus inner element separation in meters

V. CONCLUSION

The increasing demand for receivers capable of operating with multiple GNSS systems and multiple frequency bands has increased the importance of multi-band antennas. Furthermore, increasing concerns with spoofers and jammers make the spatial filtering capabilities of antenna arrays more relevant than ever within the GNSS domain. However, in practice, merging these two technologies can be challenging, as antenna array geometry is often dictated by frequency, thus, one array cannot be optimized for more than one frequency at a time. To deal with this limitation, array interpolation can be used. This work presented a study on the performance of array interpolation over multi-band antenna arrays, highlighting the performance improvement provided by array interpolation and presenting the possibility of achieving an improved inner element separation trade-off in terms of combined performance over all frequency bands received at the array. This inner element separation is shown to obtain a direction of arrival estimation bias of less than one degree for frequency bands L1, L2 and L5, simultaneously.

ACKNOWLEDGEMENTS

The research leading to the results reported in this work has received funding from the Knowledge Foundation in the framework of SafeSmart "Safety of Connected Intelligent Vehicles in Smart Cities" Synergy project (2019– 2023), Swedish Foundation for Strategic Research (SSF) in the framework of Strategic Mobility Program (2019-2020) and the ELLIIT Strategic Research Network.

REFERENCES

[1] Z. Lai, J. Yuan, X. Yang, Z. Ye, and W. Chen, "Multiband probe-fed stacked patch antenna for GNSS applications," *Progress in Electromagnetics Research Letters*, vol. 49, pp. 131–135, 2014.

[2] M. V. Heckler, M. Cuntz, A. Konovaltsev, L. A. Greda, A. Dreher, and M. Meurer, "Development of Robust safety-of-life navigation receivers," *IEEE Transactions on Microwave Theory and Techniques*, vol. 59, no. 4 PART 1, pp. 998–1005, 2011.

[3] S. Caizzone, "Miniaturized E5a/E1 Antenna Array for Robust GNSS Navigation," *IEEE Antennas and Wireless Propagation Letters*, vol. 16, pp. 485–488, 2017.

[4] Y. T. Lo, S. W. Lee, and Q. H. Lee, "Optimization of directivity and signal-to-noise ratio of an arbitrary antenna array," *Proceedings of the IEEE*, vol. 54, no. 8, pp. 1033–1045, 1966.

[5] S. Caizzone, W. Elmarissi, M. Marinho, and F. Antreich, "Direction of arrival estimation performance for compact antenna arrays with adjustable size," in *IEEE MTT-S International Microwave Symposium Digest*, 2017.

[6] M. Marinho, F. Antreich, S. Caizzone, J. da Costa, A. Vinel, and E. de Freitas, "Robust Nonlinear Array Interpolation for Direction of Arrival Estimation of Highly Correlated Signals," *Signal Processing*, vol. 144, 2018.

[7] A. Barabell, "Improving the resolution performance of eigenstructure-based direction-finding algorithms," in *ICASSP'83. IEEE International Conference on Acoustics, Speech, and Signal Processing*, vol. 8. IEEE, 1983, pp. 336–339.

[8] R. H. Roy and T. Kailath, "ESPRIT–Estimation of signal parameters via rotational invariance techniques," *Optical Engineering*, vol. 29, no. 4, pp. 296–314, 1990.

[9] B. Friedlander and A. J. Weiss, "Direction finding using spatial smoothing with interpolated arrays," *IEEE Transactions on Aerospace and Electronic Systems*, vol. 28, no. 2, pp. 574–587, 1992.